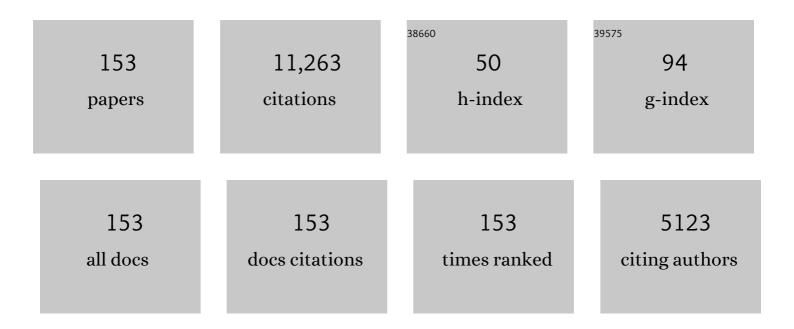
Donald C Hood

List of Publications by Year in descending order

Source: https://exaly.com/author-pdf/11432498/publications.pdf Version: 2024-02-01



#	Article	IF	CITATIONS
1	Glaucomatous damage of the macula. Progress in Retinal and Eye Research, 2013, 32, 1-21.	7.3	687
2	A framework for comparing structural and functional measures of glaucomatous damage. Progress in Retinal and Eye Research, 2007, 26, 688-710.	7.3	594
3	ISCEV standard for clinical multifocal electroretinography (mfERG) (2011 edition). Documenta Ophthalmologica, 2012, 124, 1-13.	1.0	502
4	Assessing retinal function with the multifocal technique. Progress in Retinal and Eye Research, 2000, 19, 607-646.	7.3	412
5	Automated layer segmentation of macular OCT images using dual-scale gradient information. Optics Express, 2010, 18, 21293.	1.7	239
6	Multifocal VEP and ganglion cell damage: applications and limitations for the study of glaucoma. Progress in Retinal and Eye Research, 2003, 22, 201-251.	7.3	236
7	Guidelines for basic multifocal electroretinography (mfERG). Documenta Ophthalmologica, 2003, 106, 105-115.	1.0	230
8	Retinal origins of the primate multifocal ERG: implications for the human response. Investigative Ophthalmology and Visual Science, 2002, 43, 1673-85.	3.3	216
9	Improving our understanding, and detection, of glaucomatous damage: An approach based upon optical coherence tomography (OCT). Progress in Retinal and Eye Research, 2017, 57, 46-75.	7.3	214
10	Shades of gray matter: Noninvasive optical images of human brain reponses during visual stimulation. Psychophysiology, 1995, 32, 505-509.	1.2	212
11	Structure versus Function in Glaucoma: An Application of a Linear Model. , 2007, 48, 3662.		201
12	Thickness of Receptor and Post-receptor Retinal Layers in Patients with Retinitis Pigmentosa Measured with Frequency-Domain Optical Coherence Tomography. , 2009, 50, 2328.		194
13	A comparison of the components of the multifocal and full-field ERGs. Visual Neuroscience, 1997, 14, 533-544.	0.5	186
14	Retinal Ganglion Cell Layer Thickness and Local Visual Field Sensitivity in Glaucoma. JAMA Ophthalmology, 2011, 129, 1529.	2.6	185
15	A quantitative measure of the electrical activity of human rod photoreceptors using electroretinography. Visual Neuroscience, 1990, 5, 379-387.	0.5	179
16	Blood Vessel Contributions to Retinal Nerve Fiber Layer Thickness Profiles Measured With Optical Coherence Tomography. Journal of Glaucoma, 2008, 17, 519-528.	0.8	177
17	Prevalence and Nature of Early Glaucomatous Defects in the Central 10° of the Visual Field. JAMA Ophthalmology, 2014, 132, 291.	1.4	175
18	ISCEV guidelines for clinical multifocal electroretinography (2007 edition). Documenta Ophthalmologica, 2008, 116, 1-11.	1.0	171

#	Article	IF	CITATIONS
19	A computational model of the amplitude and implicit time of the b-wave of the human ERG. Visual Neuroscience, 1992, 8, 107-126.	0.5	168
20	Initial Arcuate Defects within the Central 10 Degrees in Glaucoma. , 2011, 52, 940.		157
21	24-2 Visual Fields Miss Central Defects Shown on 10-2 Tests in Glaucoma Suspects, Ocular Hypertensives, and Early Glaucoma. Ophthalmology, 2017, 124, 1449-1456.	2.5	142
22	The Multifocal Electroretinogram. Journal of Neuro-Ophthalmology, 2003, 23, 225-235.	0.4	141
23	Light adaptation of human rod receptors: the leading edge of the human a-wave and models of rod receptor activity. Vision Research, 1993, 33, 1605-1618.	0.7	134
24	The Nature of Macular Damage in Glaucoma as Revealed by Averaging Optical Coherence Tomography Data. Translational Vision Science and Technology, 2012, 1, 3.	1.1	134
25	Measurement of Local Retinal Ganglion Cell Layer Thickness in Patients With Glaucoma Using Frequency-Domain Optical Coherence Tomography. JAMA Ophthalmology, 2009, 127, 875.	2.6	129
26	Early Glaucoma Involves Both Deep Local, and Shallow Widespread, Retinal Nerve Fiber Damage of the Macular Region. , 2014, 55, 632.		129
27	A Comparison of Fundus Autofluorescence and Retinal Structure in Patients with Stargardt Disease. , 2009, 50, 3953.		128
28	b wave of the scotopic (rod) electroretinogram as a measure of the activity of human on-bipolar cells. Journal of the Optical Society of America A: Optics and Image Science, and Vision, 1996, 13, 623.	0.8	127
29	Human cone receptor activity: The leading edge of the <i>a</i> –wave and models of receptor activity. Visual Neuroscience, 1993, 10, 857-871.	0.5	125
30	Multifocal ERG and VEP responses and visual fields: comparing disease-related changes. , 2000, 100, 115-137.		121
31	Assessment of local retinal function in patients with retinitis pigmentosa using the multi-focal ERG technique. Vision Research, 1998, 38, 163-179.	0.7	117
32	Evaluation of Inner Retinal Layers in Patients with Multiple Sclerosis or Neuromyelitis Optica Using Optical Coherence Tomography. Ophthalmology, 2013, 120, 387-394.	2.5	111
33	The Inner Segment/Outer Segment Border Seen on Optical Coherence Tomography Is Less Intense in Patients with Diminished Cone Function. , 2011, 52, 9703.		103
34	Assessing abnormal rod photoreceptor activity with the a-wave of the electroretinogram: Applications and methods. Documenta Ophthalmologica, 1996, 92, 253-267.	1.0	102
35	Identifying inner retinal contributions to the human multifocal ERG. Vision Research, 1999, 39, 2285-2291.	0.7	101
36	The 24-2 Visual Field Test Misses Central Macular Damage Confirmed by the 10-2 Visual Field Test and Optical Coherence Tomography. Translational Vision Science and Technology, 2016, 5, 15.	1.1	101

#	Article	IF	CITATIONS
37	Visual Field Defects and Multifocal Visual Evoked Potentials. JAMA Ophthalmology, 2002, 120, 1672.	2.6	100
38	Quantifying the benefits of additional channels of multifocal VEP recording. Documenta Ophthalmologica, 2002, 104, 303-320.	1.0	99
39	Enhanced S cone syndrome: Evidence for an abnormally large number of S cones. Vision Research, 1995, 35, 1473-1481.	0.7	98
40	Detecting Early to Mild Glaucomatous Damage: A Comparison of the Multifocal VEP and Automated Perimetry. , 2004, 45, 492.		98
41	A Test of a Linear Model of Glaucomatous Structure–Function Loss Reveals Sources of Variability in Retinal Nerve Fiber and Visual Field Measurements. , 2009, 50, 4254.		98
42	Phototransduction in human cones measured using the a-wave of the ERG. Vision Research, 1995, 35, 2801-2810.	0.7	97
43	Retinal Nerve Fiber Structure versus Visual Field Function in Patients with Ischemic Optic Neuropathy. Ophthalmology, 2008, 115, 904-910.	2.5	93
44	Photoresponses of human rods <i>in vivo</i> derived from paired-flash electroretinograms. Visual Neuroscience, 1997, 14, 73-82.	0.5	92
45	The Pattern Electroretinogram in Glaucoma Patients with Confirmed Visual Field Deficits. , 2005, 46, 2411.		88
46	Association Between Undetected 10-2 Visual Field Damage and Vision-Related Quality of Life in Patients With Glaucoma. JAMA Ophthalmology, 2017, 135, 742.	1.4	87
47	Regional Variations in Local Contributions to the Primate Photopic Flash ERG: Revealed Using the Slow-Sequence mfERG. , 2003, 44, 3233.		86
48	A Comparison of Progressive Loss of the Ellipsoid Zone (EZ) Band in Autosomal Dominant and X-Linked Retinitis Pigmentosa. , 2014, 55, 7417.		85
49	The Multifocal Visual Evoked Potential. Journal of Neuro-Ophthalmology, 2003, 23, 279-289.	0.4	81
50	Quantitative Electroretinogram Measures of Phototransduction in Cone and Rod Photoreceptors. JAMA Ophthalmology, 2002, 120, 1045.	2.6	79
51	Evaluation of Inner Retinal Layers in Eyes With Temporal Hemianopic Visual Loss From Chiasmal Compression Using Optical Coherence Tomography. , 2014, 55, 3328.		76
52	The Location of the Inferior and Superior Temporal Blood Vessels and Interindividual Variability of the Retinal Nerve Fiber Layer Thickness. Journal of Glaucoma, 2010, 19, 158-166.	0.8	70
53	Details of Glaucomatous Damage Are Better Seen on OCT En Face Images Than on OCT Retinal Nerve Fiber Layer Thickness Maps. , 2015, 56, 6208.		68
54	Uptake of horseradish peroxidase by frog photoreceptor synapses in the dark and the light. Nature, 1974, 249, 261-263.	13.7	67

#	Article	IF	CITATIONS
55	On improving the use of OCT imaging for detecting glaucomatous damage. British Journal of Ophthalmology, 2014, 98, ii1-ii9.	2.1	67
56	A Single Wide-Field OCT Protocol Can Provide Compelling Information for the Diagnosis of Early Glaucoma. Translational Vision Science and Technology, 2016, 5, 4.	1.1	65
57	Rates of Decline in Regions of the Visual FieldÂDefined by Frequency-Domain Optical Coherence Tomography in Patients with RPGR-MediatedÂX-Linked Retinitis Pigmentosa. Ophthalmology, 2015, 122, 833-839.	2.5	63
58	Central Glaucomatous Damage of the Macula Can Be Overlooked by Conventional OCT Retinal Nerve Fiber Layer Thickness Analyses. Translational Vision Science and Technology, 2015, 4, 4.	1.1	62
59	Automated segmentation of outer retinal layers in macular OCT images of patients with retinitis pigmentosa. Biomedical Optics Express, 2011, 2, 2493.	1.5	61
60	Method for comparing visual field defects to local RNFL and RGC damage seen on frequency domain OCT in patients with glaucoma. Biomedical Optics Express, 2011, 2, 1097.	1.5	60
61	Effects of Dystrophin Isoforms on Signal Transduction through Neural Retina: Genotype–Phenotype Analysis of Duchenne Muscular Dystrophy Mouse Mutants. Molecular Genetics and Metabolism, 1999, 66, 100-110.	0.5	58
62	Reliability of a Computer-Aided Manual Procedure for Segmenting Optical Coherence Tomography Scans. Optometry and Vision Science, 2011, 88, 113-123.	0.6	57
63	Relationships among Multifocal Electroretinogram Amplitude, Visual Field Sensitivity, and SD-OCT Receptor Layer Thicknesses in Patients with Retinitis Pigmentosa. , 2012, 53, 833.		57
64	Abnormalities of the retinal cone system in retinitis pigmentosa. Vision Research, 1996, 36, 1699-1709.	0.7	53
65	Structure-Function Agreement Is Better Than Commonly Thought in Eyes With Early Glaucoma. , 2019, 60, 4241.		53
66	The optic nerve head component of the monkey's (Macaca mulatta) multifocal electroretinogram (mERG). Vision Research, 2001, 41, 2029-2041.	0.7	52
67	FUNCTIONAL AND STRUCTURAL MEASUREMENTS FOR THE ASSESSMENT OF INTERNAL LIMITING MEMBRANE PEELING IN IDIOPATHIC MACULAR PUCKER. Retina, 2007, 27, 567-572.	1.0	51
68	Evaluation of the Structure–Function Relationship in Glaucoma Using a Novel Method for Estimating the Number of Retinal Ganglion Cells in the Human Retina. , 2015, 56, 5548.		50
69	Adaptive Optics Imaging of Healthy and Abnormal Regions of Retinal Nerve Fiber Bundles of Patients With Glaucoma. Investigative Ophthalmology and Visual Science, 2015, 56, 674-681.	3.3	50
70	Recovery kinetics of human rod phototransduction inferred from the two-branched a-wave saturation function. Journal of the Optical Society of America A: Optics and Image Science, and Vision, 1996, 13, 586.	0.8	46
71	Detecting Glaucomatous Damage with Multifocal Visual Evoked Potentials: How Can a Monocular Test Work?. Journal of Glaucoma, 2003, 12, 3-15.	0.8	46
72	Challenges to the Common Clinical Paradigm for Diagnosis of Glaucomatous Damage With OCT and Visual Fields. , 2018, 59, 788.		46

#	Article	IF	CITATIONS
73	Sites of disease action in a retinal dystrophy with supernormal and delayed rod electroretinogramb-waves. Vision Research, 1996, 36, 889-901.	0.7	44
74	A Test of a Model of Glaucomatous Damage of the Macula With High-Density Perimetry: Implications for the Locations of Visual Field Test Points. Translational Vision Science and Technology, 2014, 3, 5.	1.1	43
75	Determining abnormal latencies of multifocal visual evoked potentials: a monocular analysis. Documenta Ophthalmologica, 2004, 109, 189-199.	1.0	42
76	A comparison of retinal nerve fiber layer (RNFL) thickness obtained with frequency and time domain optical coherence tomography (OCT). Optics Express, 2009, 17, 3997.	1.7	41
77	MACULAR ATROPHY IN BIRDSHOT RETINOCHOROIDOPATHY. Retina, 2010, 30, 930-937.	1.0	41
78	Improving Glaucoma Detection Using Spatially Correspondent Clusters of Damage and by Combining Standard Automated Perimetry and Optical Coherence Tomography. , 2014, 55, 612.		41
79	A Comparison of Methods for Tracking Progression in X-Linked Retinitis Pigmentosa Using Frequency Domain OCT. Translational Vision Science and Technology, 2013, 2, 5.	1.1	40
80	Near-Infrared Autofluorescence: Its Relationship to Short-Wavelength Autofluorescence and Optical Coherence Tomography in Recessive Stargardt Disease. , 2015, 56, 3226.		40
81	Modifying the Conventional Visual Field Test Pattern to Improve the Detection of Early Glaucomatous Defects in the Central 10°. Translational Vision Science and Technology, 2014, 3, 6.	1.1	36
82	Detecting glaucoma with only OCT: Implications for the clinic, research, screening, and Al development. Progress in Retinal and Eye Research, 2022, 90, 101052.	7.3	36
83	Relating retinal nerve fiber thickness to behavioral sensitivity in patients with glaucoma: application of a linear model. Journal of the Optical Society of America Á: Optics and Image Science, and Vision, 2007, 24, 1426.	0.8	34
84	A comparison of multifocal ERG and frequency domain OCT changes in patients with abnormalities of the retina. Documenta Ophthalmologica, 2010, 120, 175-186.	1.0	33
85	Association of Glaucoma-Related, Optical Coherence Tomography–Measured Macular Damage With Vision-Related Quality of Life. JAMA Ophthalmology, 2017, 135, 783.	1.4	33
86	Determining abnormal interocular latencies of multifocal visual evoked potentials. Documenta Ophthalmologica, 2004, 109, 177-187.	1.0	32
87	Evaluation of a One-Page Report to Aid in Detecting Glaucomatous Damage. Translational Vision Science and Technology, 2014, 3, 8.	1.1	32
88	Reliability of a Manual Procedure for Marking the EZ Endpoint Location in Patients with Retinitis Pigmentosa. Translational Vision Science and Technology, 2016, 5, 6.	1.1	31
89	Four Questions for Every Clinician Diagnosing and Monitoring Glaucoma. Journal of Glaucoma, 2018, 27, 657-664.	0.8	31
90	Macular Damage, as Determined by Structure-Function Staging, Is Associated With Worse Vision-related Quality of Life in Early Glaucoma. American Journal of Ophthalmology, 2018, 194, 88-94.	1.7	30

#	Article	IF	CITATIONS
91	Quantitative Fundus Autofluorescence and Optical Coherence Tomography inABCA4Carriers. , 2015, 56, 7274.		28
92	A Region-of-Interest Approach for Detecting Progression of Glaucomatous Damage With Optical Coherence Tomography. JAMA Ophthalmology, 2015, 133, 1438.	1.4	28
93	The Locations of Circumpapillary Glaucomatous Defects Seen on Frequency-Domain OCT Scans. , 2013, 54, 7338.		27
94	A Comparison of En Face Optical Coherence Tomography and Fundus Autofluorescence in Stargardt Disease. , 2017, 58, 5227.		25
95	Confocal Adaptive Optics Imaging of Peripapillary Nerve Fiber Bundles: Implications for Glaucomatous Damage Seen on Circumpapillary OCT Scans. Translational Vision Science and Technology, 2015, 4, 12.	1.1	23
96	Technology and the Glaucoma Suspect. , 2016, 57, OCT80.		23
97	Contrast–response functions for multifocal visual evoked potentials: A test of a model relating V1 activity to multifocal visual evoked potentials activity. Journal of Vision, 2006, 6, 4.	0.1	22
98	Objective measurement of visual function in glaucoma. Current Opinion in Ophthalmology, 2003, 14, 78-82.	1.3	21
99	Deriving visual field loss based upon OCT of inner retinal thicknesses of the macula. Biomedical Optics Express, 2011, 2, 1734.	1.5	21
100	Does Retinal Ganglion Cell Loss Precede Visual Field Loss in Glaucoma?. Journal of Glaucoma, 2019, 28, 945-951.	0.8	21
101	Heterogeneity in retinal disease and the computational model of the human-rod response. Journal of the Optical Society of America A: Optics and Image Science, and Vision, 1993, 10, 1624.	0.8	20
102	An Automated Method for Assessing Topographical Structure–Function Agreement in Abnormal Glaucomatous Regions. Translational Vision Science and Technology, 2020, 9, 14.	1.1	20
103	Effectiveness of a Qualitative Approach Toward Evaluating OCT Imaging for Detecting Glaucomatous Damage. Translational Vision Science and Technology, 2018, 7, 7.	1.1	19
104	Evaluation of a Method for Estimating Retinal Ganglion Cell Counts Using Visual Fields and Optical Coherence Tomography. , 2015, 56, 2254.		17
105	Defects Along Blood Vessels in Glaucoma Suspects and Patients. , 2016, 57, 1680.		17
106	The Association Between Clinical Features Seen on Fundus Photographs and Glaucomatous Damage Detected on Visual Fields and Optical Coherence Tomography Scans. Journal of Glaucoma, 2017, 26, 498-504.	0.8	17
107	Diffuse Macular Damage in Mild to Moderate Glaucoma Is Associated With Decreased Visual Function Scores Under Low Luminance Conditions. American Journal of Ophthalmology, 2019, 208, 415-420.	1.7	17
108	Rod photoreceptor transduction is affected in central retinal vein occlusion associated with iris neovascularization. Journal of the Optical Society of America A: Optics and Image Science, and Vision, 1996, 13, 572.	0.8	16

#	Article	IF	CITATIONS
109	A comparison of structural and functional changes in patients screened for hydroxychloroquine retinopathy. Documenta Ophthalmologica, 2015, 130, 13-23.	1.0	16
110	Macular Damage in Glaucoma is Associated With Deficits in Facial Recognition. American Journal of Ophthalmology, 2020, 217, 1-9.	1.7	16
111	A method for comparing psychophysical and multifocal electroretinographic increment thresholds. Vision Research, 2002, 42, 257-269.	0.7	15
112	Rod and Cone Photoreceptor Function in Patients with Cone Dystrophy. , 2004, 45, 275.		15
113	Schisis of the Retinal Nerve Fiber Layer in Epiretinal Membranes. American Journal of Ophthalmology, 2019, 207, 304-312.	1.7	15
114	Optical Coherence Tomography Can Be Used to Assess Glaucomatous Optic Nerve Damage in Most Eyes With High Myopia. Journal of Glaucoma, 2020, 29, 833-845.	0.8	15
115	Disc Hemorrhages Are Associated With the Presence and Progression of Glaucomatous Central Visual Field Defects. Journal of Glaucoma, 2020, 29, 429-434.	0.8	15
116	Electrophysiologic imaging of retinal and optic nerve damage: the multifocal technique. Ophthalmology Clinics of North America, 2004, 17, 69-88.	1.8	13
117	Progression of Local Glaucomatous Damage Near Fixation as Seen with Adaptive Optics Imaging. Translational Vision Science and Technology, 2017, 6, 6.	1.1	13
118	Evaluation of a Qualitative Approach for Detecting Glaucomatous Progression Using Wide-Field Optical Coherence Tomography Scans. Translational Vision Science and Technology, 2018, 7, 5.	1.1	13
119	Evaluation of a Region-of-Interest Approach for Detecting Progressive Glaucomatous Macular Damage on Optical Coherence Tomography. Translational Vision Science and Technology, 2018, 7, 14.	1.1	13
120	An Evaluation of a New 24-2 Metric for Detecting Early Central Glaucomatous Damage. American Journal of Ophthalmology, 2021, 223, 119-128.	1.7	13
121	[13] Electroretinographic determination of human Rod flash response in vivo. Methods in Enzymology, 2000, 316, 202-223.	0.4	12
122	The multifocal visual evoked potential and cone-isolating stimuli: Implications for L- to M-cone ratios and normalization. Journal of Vision, 2002, 2, 4-4.	0.1	12
123	Abnormal multifocal ERG findings in patients with normal-appearing retinal anatomy. Documenta Ophthalmologica, 2011, 123, 187-192.	1.0	12
124	Detecting Glaucoma With Visual Fields Derived From Frequency-Domain Optical Coherence Tomography. , 2013, 54, 3289.		11
125	Detecting Glaucomatous Progression With a Region-of-Interest Approach on Optical Coherence Tomography: A Signal-to-Noise Evaluation. Translational Vision Science and Technology, 2018, 7, 19.	1.1	11
126	Detection of Progression With 10-2 Standard Automated Perimetry: Development and Validation of an Event-Based Algorithm. American Journal of Ophthalmology, 2020, 216, 37-43.	1.7	11

#	Article	IF	CITATIONS
127	Rod transduction parameters from the a wave of local receptor populations. Journal of the Optical Society of America A: Optics and Image Science, and Vision, 1995, 12, 2259.	0.8	10
128	OCT Circle Scans Can Be Used to Study Many Eyes with Advanced Glaucoma. Ophthalmology Glaucoma, 2019, 2, 130-135.	0.9	10
129	Strategies to Improve Convolutional Neural Network Generalizability and Reference Standards for Glaucoma Detection From OCT Scans. Translational Vision Science and Technology, 2021, 10, 16.	1.1	10
130	Global optical coherence tomography measures for detecting the progression of glaucoma have fundamental flaws. Eye, 2021, 35, 2973-2982.	1.1	10
131	The OCT RNFL Probability Map and Artifacts Resembling Glaucomatous Damage. Translational Vision Science and Technology, 2022, 11, 18.	1.1	10
132	A Topographic Comparison of OCT Minimum Rim Width (BMO-MRW) and Circumpapillary Retinal Nerve Fiber Layer (cRNFL) Thickness Measures in Eyes With or Suspected Glaucoma. Journal of Glaucoma, 2020, 29, 671-680.	0.8	9
133	Association of Patterns of Claucomatous Macular Damage With Contrast Sensitivity and Facial Recognition in Patients With Claucoma. JAMA Ophthalmology, 2021, 139, 27.	1.4	9
134	Rod photoreceptor temporal properties in retinitis pigmentosa. Experimental Eye Research, 2011, 92, 202-208.	1.2	8
135	Unilateral retinopathy secondary to occult primary intraocular lymphoma. Documenta Ophthalmologica, 2013, 127, 261-269.	1.0	8
136	Comparison of Widefield and Circumpapillary Circle Scans for Detecting Glaucomatous Neuroretinal Thinning on Optical Coherence Tomography. Translational Vision Science and Technology, 2018, 7, 11.	1.1	8
137	Variability and Power to Detect Progression of Different Visual Field Patterns. Ophthalmology Glaucoma, 2021, 4, 617-623.	0.9	7
138	Electrophysiology. Ophthalmology Clinics of North America, 2003, 16, 237-251.	1.8	6
139	Imaging Glaucoma. Annual Review of Vision Science, 2015, 1, 51-72.	2.3	5
140	On relating physiology to sensation. Behavioral and Brain Sciences, 1981, 4, 195-195.	0.4	4
141	Qualitative evaluation of neuroretinal rim and retinal nerve fibre layer on optical coherence tomography to detect glaucomatous damage. British Journal of Ophthalmology, 2020, 104, 980-984.	2.1	4
142	Detecting Progression in Advanced Glaucoma: Are Optical Coherence Tomography Global Metrics Viable Measures?. Optometry and Vision Science, 2021, 98, 518-530.	0.6	4
143	The 24-2 Visual Field Guided Progression Analysis Can Miss the Progression of Glaucomatous Damage of the Macula Seen Using OCT. Ophthalmology Glaucoma, 2022, 5, 614-627.	0.9	4
144	Auto-immune-like cone dystrophy. Documenta Ophthalmologica, 2004, 109, 215-221.	1.0	3

#	Article	IF	CITATIONS
145	Deep Defects Seen on Visual Fields Spatially Correspond Well to Loss of Retinal Nerve Fiber Layer Seen on Circumpapillary OCT Scans. , 2018, 59, 621.		3
146	Did the OCT Show Progression Since the Last Visit?. Journal of Glaucoma, 2021, 30, e134-e145.	0.8	3
147	Abnormal Rod Photoreceptor Function in Retinitis Pigmentosa. , 1995, , 359-370.		3
148	Association of Macular Optical Coherence Tomography Measures and Deficits in Facial Recognition in Patients With Glaucoma. JAMA Ophthalmology, 2021, 139, 486.	1.4	2
149	Author Response: Challenges to the Common Clinical Paradigm for Diagnosis of Glaucomatous Damage With OCT and Visual Fields. , 2018, 59, 5524.		1
150	Reply. Ophthalmology, 2018, 125, e27-e28.	2.5	0
151	The Use of Multifocal Electroretinograms and Multifocal Visual Evoked Potentials in Optic Nerve Disorders. , 2014, , 325-351.		Ο
152	The Use of Multifocal Electroretinograms and Visual Evoked Potentials in Diagnosing Optic Nerve Disorders. , 2007, , 245-269.		0
153	Structure–function analysis for macular surgery in patients with coexisting glaucoma. Graefe's Archive for Clinical and Experimental Ophthalmology, 2021, , 1.	1.0	Ο